Proceedings of the 26th International Conference on
Port and Ocean Engineering under Arctic Conditions
June 14-18, 2021, Moscow, Russia

Scale-model ridges and interaction with narrow structures, Part 3 Analysis of Ridge Keel Punch Tests

Jaakko Heinonen[1], Maria Tikanmäki[1], Eeva Mikkola[1], Ilkka Perälä[1], Aleksey Shestov[2], Knut V. Høyland[3], Evgenii Salganik[3], Marnix van den Berg[3], Hongtao Li[3], Zongyu Jiang[3,5], Åse Ervik[4], Otto Puolakka[5]

[1] *VTT Technical Research Centre of Finland Ltd.*
[2] *UNIS, Norway*
[3] *NTNU, Norway*
[4] *Multiconsult, Norway*
[5] *Aalto University, Finland*

ABSTRACT

An experimental campaign to investigate sea ice ridge interaction with bottom-fixed structures was carried out in the Aalto ice tank in Espoo Finland in August, 2019. The aim was to investigate a) the scaled ridge properties, b) the ice processes during testing and c) the scaling of ridge forces with respect to a cylindrical and a conical structure at the water line. This presentation focuses on analyzing ridge keel punch tests. In a punch test, a circular platen of consolidated layer is first cut free from the surrounding ice field. Thereafter, the ice is pushed vertically downwards with a cylindrical indentor to break the underlying keel. The measured load-displacement relationship can be used for the evaluation of the mechanical properties of rubble. Three ice sheets were created and used to build ridges, in which the ridge consolidation temperature and time were varied. All together 24 punch tests were carried out, whereas 14 of them were done for consolidated ridge, six for unconsolidated ridge, three for surrounding level ice and one in the open water to determine the buoyancy load on the indentor. Both the structural tests and punch tests showed clearly that the ridge strength and load depend strongly on the consolidation.

KEY WORDS: ice loads; ridge loads; punch tests; offshore wind turbine; ice rubble; ridge keel

INTRODUCTION

In cold sea areas, like the Gulf of Bothnia, sea freezes annually and the sea ice introduces a major load scenario for offshore structures. Increasing activities regarding wind energy production in ice-covered sea areas require cost-effective solutions for wind turbine support structures. Narrow structures, like monopiles, are commonly used for shallow sea areas (water depth max. ~30 m). A conical shape at the waterline is often used in ice-infested sea areas, because it induces the level ice to fail by bending instead of crushing. The cone is a reasonable structural concept to mitigate both the level ice loads and ice-induced vibrations. However, the situation is not that straightforward when an ice ridge interacts with the conical structure. Even though the cone breaks the consolidated layer effectively, the undelaying keel interacts with a wider geometry as in the case of monopile resulting in higher keel loads. Therefore, in areas where ridges are probable ice features, it is important to take into account these disadvantages when considering whether the cone is a suitable structural concept.

Ice ridges are common features in the Northern seas and they often introduce a dominating loading scenario for the Ultimate Limit State (ULS) design. However, there are no definite guidelines to evaluate ridge loads on conical structures. Serre and Liferov (2010) approached this challenge by studying ridge interaction in the model basin with the cone angle of 62 degrees. Based on experimental tests and advanced numerical simulation, Serre and Liferov concluded that "ISO recommendations are insufficient and potentially under-conservative with regard to calculation of loads from wide ridge keels on simple conical structures."

An experimental campaign to investigate sea ice ridge interaction with bottom-fixed structures was carried out in the Aalto ice tank in Espoo Finland in August, 2019. The aim was to investigate a) the scaled ridge properties, b) the ice growth, consolidation and failure processes and c) the scaling of ridge forces with respect to a cylindrical and conical structures at the water line. An overview of tests was introduced by Shestov et al. (2020) and the analysis of thermal consolidation by Salganik et al. (2021) and the analysis of ridge loads on structures by Jiang et al. (2021). This presentation concentrates on the analyses of ridge keel punch tests to characterize the mechanical properties of the ice rubble in the ridge keel.

TEST SET-UP

The tests were part of the EU's HYDRALAB+ program and they were carried out in the Aalto Ice Tank, the facility in the Aalto University. The size of the rectangular ice basin is 40 m times 40 m with 2.8 m water depth. The ice tank is equipped with a cooling system and a carriage with an instrument wagon. The model ice for ridge creation was granular fine-grained ice produced by spraying the basin water from the moving carriage at -10°C.

The test program consisted of following main steps:

1) Growing an ice sheet by spraying water in cold temperature.
2) Production of a ridge by breaking the ice sheet mechanically into pieces to form a ridge
3) Consolidating the ridge by adjusting the air temperature in the basin with a specific cold temperature cycle
4) Measure the mechanical properties of ice and geometry prior to an ridge-structure interaction experiment.
5) Run the ridge interaction experiment with a cylindrical and conical structures (cone angle 75°).
6) Profiling the ridge keel geometry and testing the mechanical properties of ice rubble.

During the campaign altogether three different ice sheets and ridges were created. The initial ice temperature and accumulated air temperatures during consolidation (Freezing Degree Hours) were varied to study the how the consolidation affects the model-scaled ridge properties. All three ridges were consolidated slightly different way. After the ridge formation, the first ridge was consolidated over the night before testing. One half of the second and third ridge were first studied without consolidation and thereafter the second half was left over the night for consolidation and studied in the next day by the structural and mechanical tests.

Ridge consolidation was studied by using the thermistor strings to measure the temperature profile and temporal changes of ridge in the vertical direction (Salganik et al., 2021). This information was used to estimate the thickness of the consolidated layer and to study whether the consolidation correlates with the rubble strength.

The model ice in each ice sheet was characterized by various measurements: ice density, salinity, flexural strength and compressive strength. Several punch shear tests were carried out to characterize the rubble strength related to each ridge-structure interaction test.

A schematic drawing of a ridge interaction test is shown in Fig. 1a. The structures, shown in Fig. 1b, were fixed to the main carriage of the ice basin. The carriage was moved with a constant velocity through the ridges. Global ice forces on the structure were measured by a six DOF load cell connected to the structure. In addition, tactile sensors were used to measure the contact pressure of ice. The experiments were filmed above the water level and underwater with 3D camera set-up (Shestov et al., 2020, Jiang et al., 2021). Punch tests were carried out between the channels created in the structural tests and between the channel and the side wall of the ice tank as schematically shown in Figure 1. Ridge keel thickness profile was measured nearby the areas of punch tests.

In a punch test, a circular platen of consolidated layer is first cut free from the surrounding ice field (Figure 2). Thereafter, the ice is pushed vertically downwards with a cylindrical indentor (diameter 50 cm) to break the underlying keel (keel depth 35 - 50 cm). When the indentor moves downwards, the ice rubble starts to deform and fail along inclined shear failure zone, as illustrated in Figure 2. At same time the ice rubble may compact under the indentor. The measured load-displacement relationship can be used for the evaluation of the mechanical properties of rubble.

All together 24 punch tests were carried out, whereas 14 of them were conducted for consolidated ridge, six for unconsolidated ridge, three for surrounding level ice and one in the open water to

determine the buoyancy load on the indentor. Several punch tests were analyzed for each ridge as listed in Table 1. Some of the tests were carried out without preliminary cut through the consolidated layer.

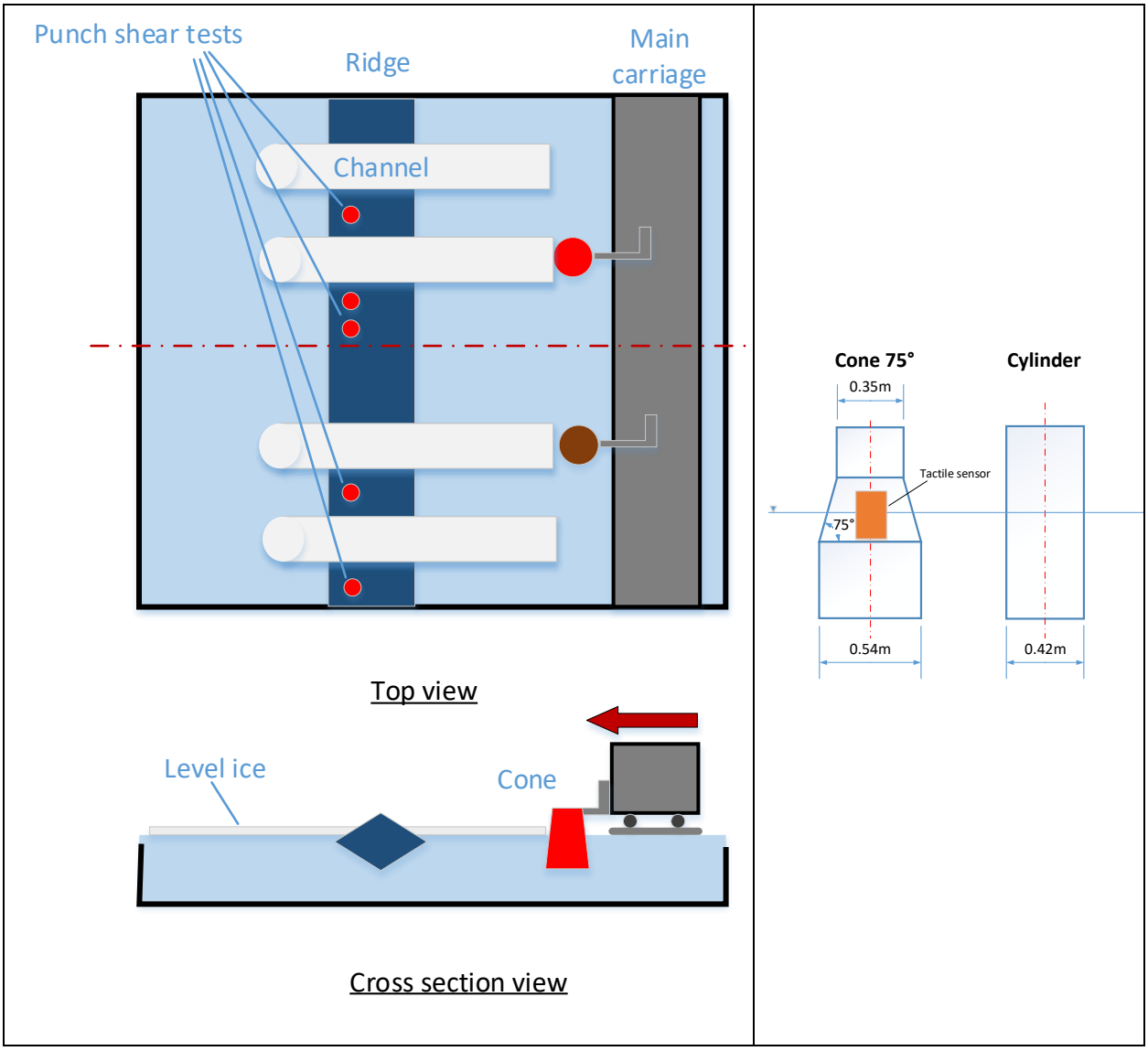

Figure 1. Left: Layout of the test arrangements in the ice basin. Right: Shape and main dimensions of the test structures in the model scale.

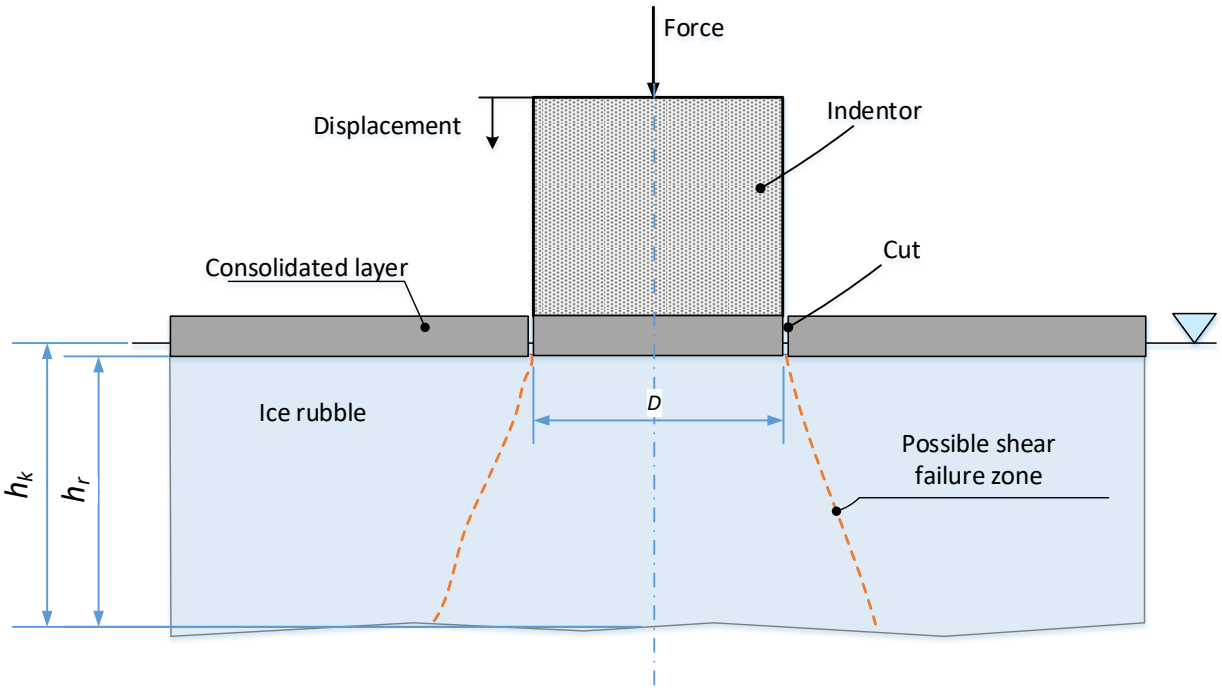

Figure 2. Schematic sketch of the punch shear test. Indentor diameter was 50 cm.

TEST RESULTS

A list of punch tests is shown in Table 1 giving information about whether the ridge was consolidated before the punch test or not, and whether the consolidated layer was cut around the indentor or not.

Table 1. List of punch tests carried out in the ice basin with maximum loads. CL is abbreviation for the consolidated layer.

Punch test	Date	Ridge			Fmax (N)
1	23.8.2019	#1	CL cut	consolidated	332
2	23.8.2019		CL cut		577
3	23.8.2019		CL cut		491
4	23.8.2019		CL cut		551
5	23.8.2019		CL cut		547
6	23.8.2019		no cut		618
7	23.8.2019		no cut		750
8	23.8.2019		Level ice punch		519
9	23.8.2019		Open water punch		800
10	26.8.2016	#2	CL cut	no consolidation	no peak
11	26.8.2016		CL cut		no peak
12	26.8.2016		CL cut		no peak
13	27.8.2019	#2	CL cut	consolidated	746
14	27.8.2019		CL cut		669
15	27.8.2019		Level ice punch		1061
16	29.8.2019	#3	CL cut	no consolidation	no peak
17	29.8.2019		no cut		no peak
18	29.8.2019		no cut		no peak
19	29.8.2019		Level ice punch		188
20	30.8.2019	#3	CL cut	consolidated	389
21	30.8.2019		CL cut		388
22	30.8.2019		CL cut		381
23	30.8.2019		CL cut		372
24	30.8.2019		no cut		518

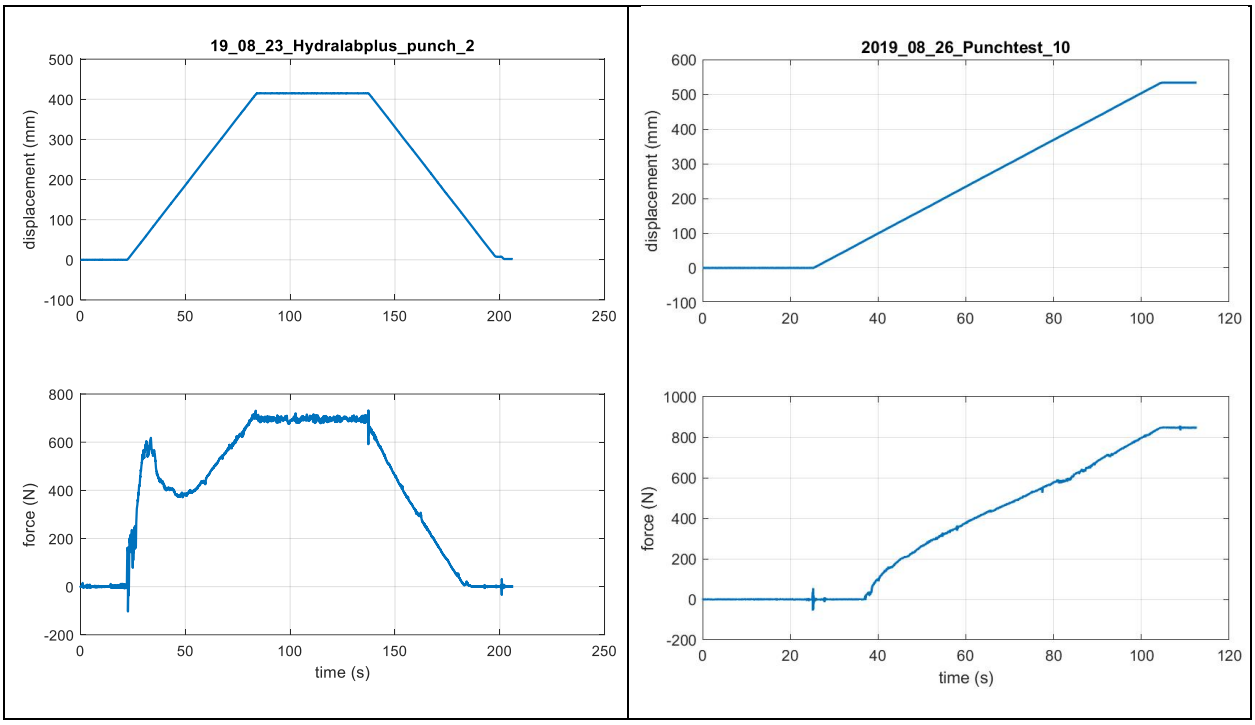

Figure 3. Examples of the indentor's force and displacement time history curves from the punch tests when the consolidated layer was cut around the indentor. Left: Punch test #2 in the consolidated ridge. Right: Punch test #10 in the unconsolidated ridge.

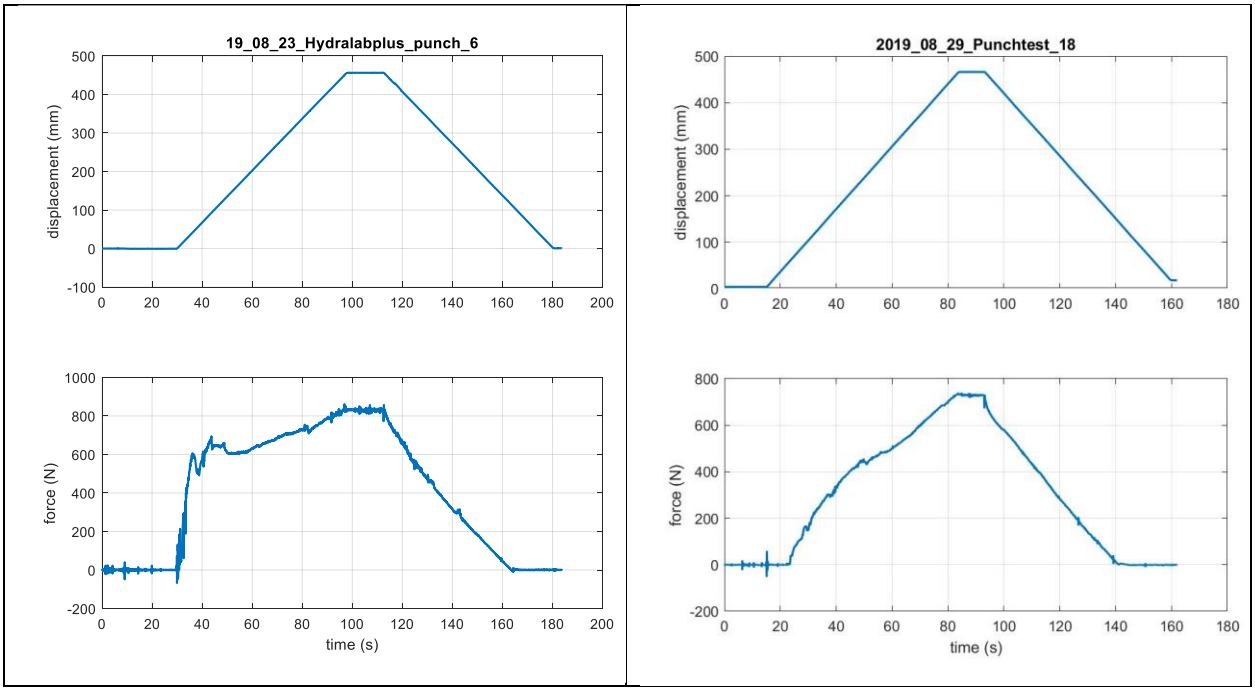

Figure 4. Examples of the indentor's force and displacement time history curves from the punch tests without cutting the consolidated layer beforehand. Left: Punch test #6 in the consolidated ridge. Right: Punch test #18 in the unconsolidated ridge.

Time history curves of punch load presented in Figure 3 and Figure 4 show clear difference between the consolidated and unconsolidated ridges.

For the consolidated ridge, one may recognize following phases from the load pattern (left hand side curves in Figure 3 and Figure 4):
- The load increases until the ice rubble starts to fail. Some small load variations, i.e. load peaks, occur due to local failures like the breakage of an ice block or freeze bond
- The global load maximum in the loading period clearly indicates the breakage of the ice rubble
- The softening phase when the load decreases. The load is contributed by the combined effect of the frictional resistance and the buoyancy of ice rubble.
- thereafter the measured punch load increases again due to buoyancy of submerged indentor.

For the unconsolidated ridge, the load signal showed only small variation from linearly increasing trend (Figure 4 right). The load is mostly contributed by the buoyancy of the ice rubble and submerged indentor. Slight increase in the load is due to frictional resistance of the ice rubble (time period from start to 55 s in Punch Test #18). No clear peaks in the load pattern can be observed.

The load patterns were fairly similar, independently whether the consolidated layer was cut beforehand or not. However, when the consolidated layer was not cut beforehand, the load drop after the global failure was not as clear. In this case wider area of the consolidated layer between the indentor and ice rubble was stucked between the indentor and underlying ice rubble. Consequently, the breaking of the consolidated layer contributed some load.

ANALYSIS

The load capacity in the punch test depends on the geometrical dimensions of the keel and the loading indentor and the strength of ice rubble. The latter is strongly governed by the internal structure of ice rubble and thermal consolidation.

We start our analyses of ridge strength by a simple prediction. An approximation of the shear strength in the keel is based on the assumption that the keel collapses along a cylindrical failure surface. The average shear strength along the failure surface can then be estimated as

$$\tau = \frac{F_{\max} - B}{\pi D h} \tag{1}$$

where h is the effective thickness of the keel and D is the diameter of the platen. Fmax is measured peak load during the punch test. B is the buoyancy load defined following:

$$B = \gamma V + \rho_w g A z = \frac{\pi D^2}{4}\left(\gamma h + \rho_w g z\right) \tag{2}$$

where the first term describes the buoyancy of the mobilized ice rubble under the indentor and the second term is the buoyancy load induced when the indentor moves downwards and penetrates the water level replacing some of the water. γ is buoyant force of ice rubble defined as

$$\gamma = (\rho_w - \rho_i)(1-\eta)g \tag{3}$$

where ρ_w is density for water and ρ_i is density for the ice blocks. η is the relative volume of water pockets in the rubble (macro porosity). g is the gravitative acceleration (g = 9.81 m/s^2).

When the ice rubble is assumed to behave like cohesive-frictional material, one may use Mohr-Coulomb (MC) criterion to estimate the rubble failure, which is also widely used in geotechnical engineering. In the Mohr-Coulomb criterion the rubble strength is described by the cohesion and internal friction. The to the Mohr-Coulomb yield criterion is written as

$$|\tau| = c - p\tan(\phi) \tag{4}$$

where c is the cohesion and φ is the angle of internal friction, and p is the pressure (normal stress) affecting the failure surface. Based on passive soil pressure theory, one may define the passive earth resultant force P_p as

$$P_p = \frac{1}{2}K_p\gamma h^2 \tag{5}$$

where K_p is the coefficient of passive pressure. By assuming the keel failure along the cylindrical surface, the coefficient of passive pressure reduces to

$$K_p = \frac{1+\sin(\varphi)}{1-\sin(\varphi)} = \tan^2\left(45^\circ + \frac{\varphi}{2}\right) \tag{6}$$

The punch load capacity for the cylindrical failure mode can be found as

$$F = cA_c + \frac{1}{2}K_p h^2 A_c \tan(\varphi) + B \tag{7}$$

where the maximum load F is divided into three parts: the first term is the cohesive part, the second is the frictional part and the last one is the buoyancy load.

Because there are two unknown strength parameters – cohesion and friction angle – we carry out a parametric study to determine admissible combinations of them. This is achieved by comparing the measured punch load with analytical calculations. By plotting the maximum force versus cohesion and the measured load capacity in the same plot (Figure 5), the points where the simulated and the measured lines crosses represent admissible combinations of cohesion and the friction angle. This procedure was then repeated for each test case resulting in curves representing the cohesion versus the friction angle, as shown in right hand side in Figure 5. From these contour curves one may determine admissible combination of the cohesion and friction angle resulting in same load capacity of the ridge keel as measured.

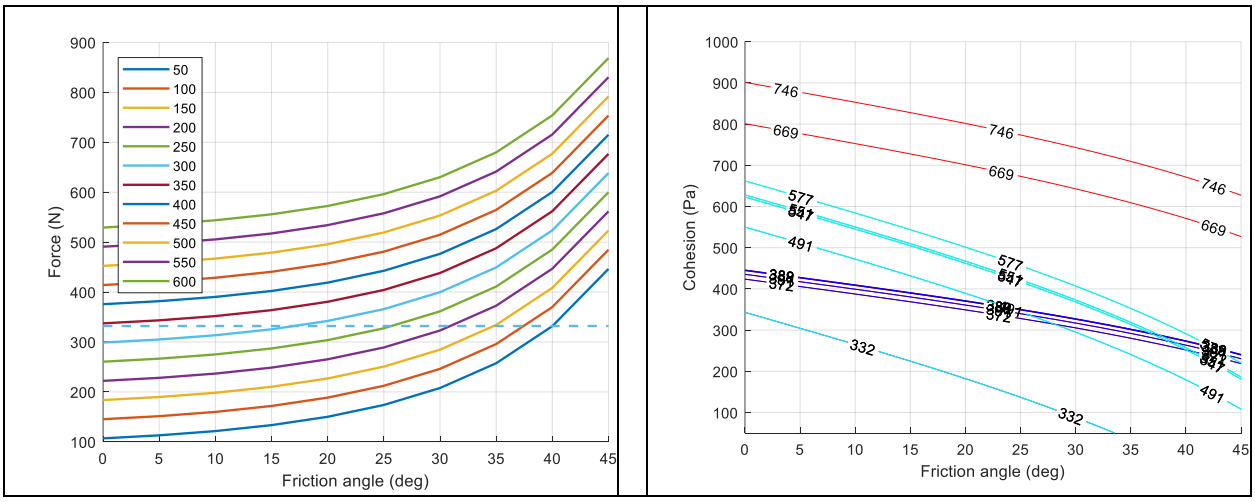

Figure 5. Left: Maximum punch force versus internal friction angle with different values for the cohesion. Dashed line shows maximum measured load in Test #1. Right: Contour lines of maximum measured loads shown in Table 1 as functions of the cohesion and the friction angle. Cyan colored lines are from Ridge #1, red lines from Ridge #2 and blue lines from Ridge #3.

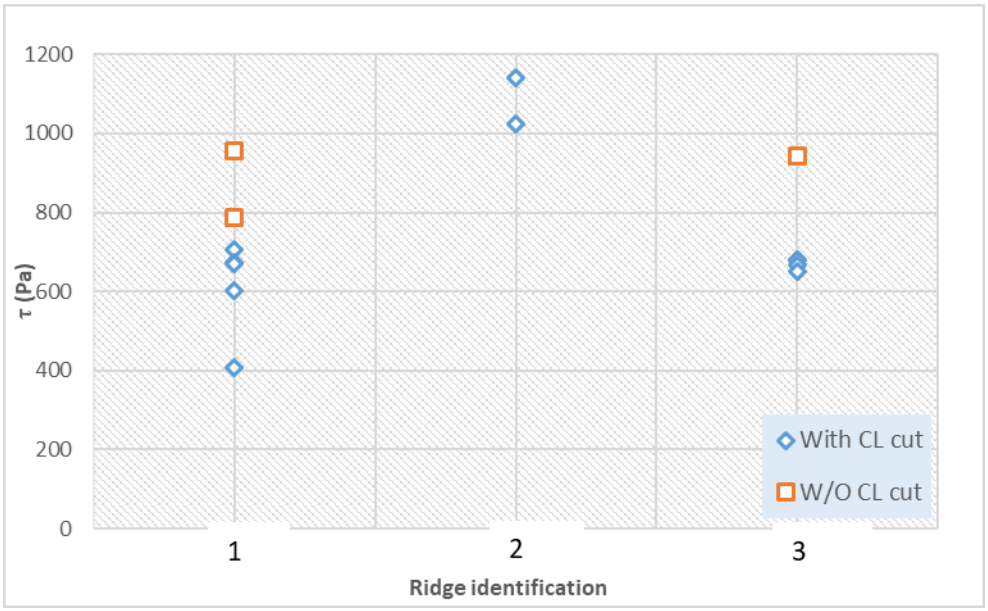

Figure 6. Shear strength of ice rubble determined from punch tests in three different consolidated ridges.

DISCUSSION

Ice rubble strength in various ridges were first predicted by comparing the average shear strength. For the consolidated ridge, the shear strength varied between 407 and 1142 Pa and the average was 756 Pa. Even though the variation is significant compared to the average value, this simple estimate showed clearly Ridge 1 (average 612 Pa) and Ridge 3 (average 669 Pa) to be much weaker than

Ridge 2, in which the average shear strength based on two measurements was 1083 Pa. All these values are based on the case when the consolidated layer was cut around the indentor. Even though the maximum loads in Ridge 2 were not much higher, the keel depth was smaller than in Ridge 1. Combined effect from higher loads and lower thickness resulted in high increase of the shear strength. The same trend between the ridges was shown by the passive pressure theory as seen in the admissible combinations of the cohesion and the friction angle (Figure 5 right). The red lines in Figure 5 (right) corresponding to Ridge 2 is significantly stronger in terms of cohesion compared to Ridges 1 and 3.

The difference between two ridges is well in line with the thermal consolidation study (Salganik et al. 2021). Ridge 2 was consolidated more in terms of Freezing Degree Hours than Ridge 1 and 3, resulting in stronger freeze bonds in the ice rubble making also the ice rubble stronger.

Even though the load patterns were fairly similar regardless of whether the consolidated layer was cut beforehand or not, the punch load and correspondingly the keel strength were generally higher without cutting the consolidated layer. This indicates the formation of refrozen layer that was strong to break. In this case the punch tests do not solely measure the strength of ice rubble.

From earlier studies of full-scale punch tests in the Baltic Sea (Heinonen, 2004), the estimation of the shear strength of ice rubble varied from 4.2 to 20.3 kPa between different winters (1999-2001). By comparing this to model-scale values regarding different ridges, we conclude the average shear strength ratio equal to 12 (full-scale/model-scale). Range of the shear strength scale-ratio can be predicted by comparing first Ridge 1 to the lowest value in the full-scale, i.e. 4.2 kPa to 612 Pa. Similarly, we may compare Ridge 2 to the highest value in the full-scale, i.e. 20.3 kPa to 1083 Pa. The range is therefore between 7 and 19.

When comparing the cohesive-frictional material properties in the full-scale and model-scale, one may compare the value of cohesion when the friction angle is kept constant. We chose the friction angle equal to 25º. Full-scale values of Mohr-Coulomb cohesion vary in the range of 5 - 11 kPa (Heinonen, 2004), while model-scale vary in the range of 350 -780 Pa (the lowest value 130 Pa was ignored). Range of the cohesion scale-ratio becomes equal to 14.

In full-scale ridges in the Baltic Sea, the diameter of indentor varied between 2.5 and 4.7 m. The keel depths varied between 3.0 and 6.4 m. Corresponding values in the model-scale were the diameter 0.5 m and the keel depth 0.35 - 0.5 m. The geometrical scale is therefore in the range of 5 - 13. One may conclude the strength scales in the ice rubble (average in shear strength 12 and cohesion 14) in measured ridges are to some extent in the same range as the geometrical scale (range 5 - 13).

These analytical methods give a straightforward way for first impression about the ridge keel strength. One should pay attention that both models used here are based on previously chosen failure mechanisms. For the simplicity, here we used cylindrical shear plug failure. Based on earlier studies, the keel fails typically along inclined failure zones. In addition some compaction of ice rubble may take place. To consider all these effects, one needs to apply numerical methods to simulate progressive failure process during the test, *c.f.* Heinonen and Høyland (2013). This is left for the future study.

CONCLUSIONS

Three ice sheets were created and used to build ridges in the model ice basing, in which the ridge consolidation temperature and time were varied. Several punch tests were analyzed for each ridge. In a punch test, a circular platen of consolidated layer was first cut free from the surrounding ice field. However, some of the tests were carried out without preliminary cut through the consolidated layer. Thereafter, the ice is pushed vertically downwards with a cylindrical indentor (diameter 50 cm) to break the underlying keel (keel depth 35 - 50 cm). The measured load-displacement relationship was used for the evaluation of the mechanical properties of rubble.

We used two alternative models to predict the strength of ice rubble: firstly, a simplified method to determine the shear strength and secondly, using the passive soil pressure theory to determine Mohr-Coulomb material parameters: cohesion and friction angle.

When comparing the strength of ice rubble in measured ridges, both theoretical models showed clearly, that the strength of ice rubble depends strongly on the consolidation time. Ridge #2 was stronger than the others mostly due to harder consolidation in terms of Freezing Degree Hours.

When comparing the model-scale results to available full-scale results, one may conclude the strength scales in the ice rubble (average in shear strength 12 and cohesion 14) in measured ridges are to some extent in the same range as the geometrical scale (range 5 - 13).

ACKNOWLEDGMENTS

The authors gratefully acknowledge the EU's Horizon 2020 Research and Innovation Programme of the Integrated Infrastructure Initiative HYDRALAB+, Contract no. 654110. The authors would also like to thank the crew in the Aalto ice basin: Teemu Päivärinta and Lasse Turja for their efforts for preparing and carrying out the tests.

The authors gratefully acknowledge the Academy of Finland for funding the SmartSea project (Strategic research programme [grant numbers 292985 and 314225]).

REFERENCES

Heinonen, J., Constitutive Modeling of Ice Rubble in First-Year Ridge Keel, VTT Publications 536, Espoo 2004, 142 p., Doctoral thesis, ISBN 951-38-6930-5 (sort back ed.), URL: http://www.vtt.fi/inf/pdf/publications/2004/P536.pdf

Heinonen, J., Høyland. K.V., 2013, Strength and Failure Mechanisms in Scale-Model Ridge Keel Punch through Tests - FE-Analysis, Proceedings of the 22nd International Conference on Port and Ocean Engineering under Arctic Conditions, June 9-13, 2013, Espoo, Finland

Shestov, A., Ervik, A., Heinonen J., Perälä, I., Høyland K.V., Salganik E., Li, H., van den Berg, M., Jiang, Z., Puolakka, O., 2020. Scale-model ridges and interaction with narrow structures, Part 1: Overview and scaling. *In Proceedings of the 25th IAHR International Symposium on Ice*. Trondheim, Norway. June 14-18, 2020. International Association for Hydro-Environment Add Engineering and Research (IAHR).

Salganik, E., Ervik, Å, Heinonen, J., Høyland, K.V, Perälä, I., Puolakka, O., Shestov, A., van den Berg. M. 2021. Scale-model ridges and interaction with narrow structures, Part 2: thermodynamics of ethanol ice. In Proceedings of the 26th International Conference on Port and Ocean Engineering under Arctic Conditions (POAC 2021)

Serré, N., Liferov, P., 2010. Loads from ice ridge keels - experimental vs. numerical vs. analytical. In: Proc. of the 20 Int. Symp. on Ice (IAHR), Lahti, Finland. Paper # 92.

Zongyu Jiang, Heinonen, J., Tikanmäki, M., Mikkola, E., Perälä, I. Shestov, A., Høyland, K.V. Salganik, E., van den Berg, M., Li, H., Ervik, Å., Puolakka, O. 2021. Scale-model ridges and interaction with narrow structures, Part 4 Global loads and failure mechanisms. In Proceedings of the 26th International Conference on Port and Ocean Engineering under Arctic Conditions (POAC 2021)